

The electronic structure of C₆₀/ZnPc interface for organic photovoltaic device with blended layer architecture

S. H. Park,¹ J. G. Jeong,¹ Hyo-Jin Kim,¹ Seung-Han Park,¹ Mann-Ho Cho,^{1,a)}
Sang Wan Cho,² Yeonjin Yi,³ Min Young Heo,⁴ and Hyunchul Sohn^{4,a)}

¹*Institute of Physics and Applied Physics, Yonsei University, Seoul 120-749, Republic of Korea*

²*Department of Physics, Boston University, 590 Commonwealth Avenue, Boston, Massachusetts 02215, USA*

³*Division of Industrial Metrology, KRISS, Daejeon 305-340, Republic of Korea*

⁴*Department of Ceramic Engineering, Yonsei University, Seoul 120-749, Republic of Korea*

(Received 15 July 2009; accepted 15 December 2009; published online 4 January 2010)

The interfacial electronic structures of fullerene (C₆₀)/zinc-phthalocyanine (ZnPc) and C₆₀/ZnPc:C₆₀ (50 wt %) containing a blended layer were investigated by *in situ* ultraviolet photoelectron spectroscopy (UPS), in an attempt to understand the role of the blended layer in improving the performance of organic photovoltaic devices that contain such layers. From the UPS spectra, the band bending found to be 0.30 eV in the ZnPc layer and 0.43 eV in the C₆₀ layer at the C₆₀/ZnPc interface. On the other hand, the band bending was 0.25 eV in both of the organic layers at the ZnPc:C₆₀/ZnPc interface and no significant band bending in the C₆₀ layer at the C₆₀/ZnPc:C₆₀ interface was found. The observed interface dipole was 0.06 eV at the C₆₀/ZnPc interface and 0.26 eV at the ZnPc:C₆₀/ZnPc interface. The offset between the highest unoccupied molecular orbital of ZnPc and the lowest occupied molecular orbital of C₆₀ was 0.75 eV at C₆₀/ZnPc and was 1.04 eV at the ZnPc:C₆₀/ZnPc interface. The increased offset can be attributed to an increase in the interface dipole, caused by the blending donor and acceptor material. The blending facilitates charge transfer between the donor and acceptor, resulting in an increase in the interface dipole, resulting in a larger offset. © 2010 American Institute of Physics.

[doi:10.1063/1.3285174]

Since the observation in 1906 by Pochettino,¹ that certain types of organic materials show photoconductivity, organic photovoltaic (OPV) devices have been a subject of considerable attention, because of their potential benefits and low cost, flexibility, and variety of possible applications.^{2–4} Extensive efforts have been made to improve the power conversion efficiencies of OPVs by maximizing the energy difference between the highest occupied molecular orbital (HOMO) of the donor and the lowest unoccupied molecular orbital (LUMO) of the acceptor to increase open circuit voltage (V_{oc}) (Ref. 5) and by inserting an electron (hole) blocking layer for higher short circuit currents (I_{sc}),⁶ and modifying the interface structure to overcome the short exciton diffusion length of organic materials.⁷ One of the widely used methods for improving the interface structures of bilayer OPVs is the introduction of a blended region at the donor-acceptor (DA) interface in order to increase the DA interface area, so as to overcome the short diffusion length of an exciton.⁸

The OPV performance is strongly dependent on the electronic structures of the organic interface. While studies have focused on the energy level offset between the donor HOMO and the acceptor LUMO, the interfacial electronic structure between donor and acceptor layers in OPV is less well understood. Furthermore, band alignment cannot be successfully explained using the common vacuum level concept when an organic interface is present and the same is true for the case of a blended heterojunction. Changes in interface electronic structures as the result of the presence of a blended

layer have not been considered, although the interfacial electronic structure can differ from that of a bilayer heterojunction structure. In recent studies, the preparation of OPVs using zinc-phthalocyanine (ZnPc) and fullerene (C₆₀) have been reported because of the appropriate band gap and desirable absorption properties of ZnPc and the large electron affinity of C₆₀. These OPVs showed a power conversion efficiency of 1.2%–3.6% and a V_{oc} of 0.44–0.57 V, when a blended heterojunction structure was used.^{9,10} However, the issue of how V_{oc} is improved by a blended layer is not clearly understood at this time.

In this study, we investigated the detailed electronic structure and the energy level alignments at a C₆₀/ZnPc interface and the same interface, prepared with an inserted blended layer by using ultraviolet photoemission spectroscopy (UPS). UPS has been used extensively to determine the electronic structure at interfaces between an organic layer and either a metal or a second organic layer.¹¹ Our results show that the blended layer causes a change in electronic structure at the interface, which would likely affect device performance. Charge transfer between donor and acceptor at the interface were determined from changes in HOMO and the secondary electron (SE) cutoff position during the step-by-step deposition sequence.

ITO coated glass substrates were cleaned by ultrasonic treatment in de-ionized water, a dilute solution of glass cleaner, and pure ethanol, and then sputter cleaned in an analysis chamber for 5 min. Commercial samples of ZnPc and C₆₀ were obtained from Aldrich (both sublimed grade). We prepared series of multilayer films of C₆₀/ZnPc/ITO and C₆₀/ZnPc:C₆₀ (50 wt %)/ZnPc/ITO in a deposition chamber that was directly connected to the analysis chamber to carry

^{a)}Authors to whom correspondence should be addressed. Electronic addresses: mh.cho@yonsei.ac.kr and hyunchul.sohn@yonsei.ac.kr.

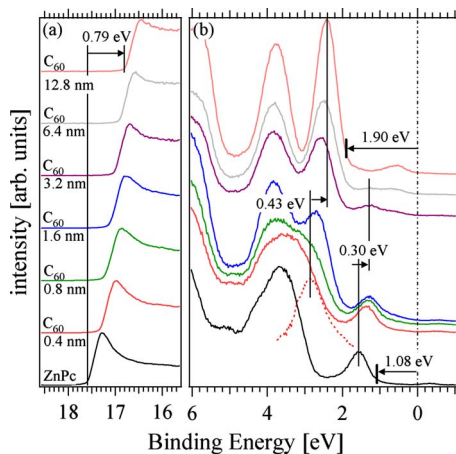


FIG. 1. (Color online) UPS spectra collected near the secondary cutoff region (a) and the Fermi level (b) during the step-by-step layer deposition of C_{60} on the ZnPc layer. The HOMO shift of ZnPc is 0.30 eV, that of C_{60} is 0.43 eV and SE cutoff position is also moved 0.79 eV to lower binding energy.

out the *in situ* measurements. [We use the notation (top layer)/(bottom layer) unless indicated.] The C_{60} and ZnPc: C_{60} blend layers were deposited in a stepwise manner on the a 20 nm thick ZnPc deposited on ITO substrate. The blend layer was prepared by the coevaporation of ZnPc and C_{60} . All organic materials were evaporated using a thermal deposition technique. The thickness of each layer was monitored by means of a calibrated quartz crystal thickness monitor. The analysis chamber was equipped with a hemispherical electron energy analyzer (PHI 5700 spectrometer), a standard x-ray source (Al $K\alpha$, 1486.6 eV) and an unfiltered UV (He I, 21.2 eV) source. A -15 V of sample bias was applied to measure the work function of the sample. The analysis and deposition chamber were maintained at pressures of at least 3×10^{-9} and 3×10^{-8} Torr, respectively. The energy scale of presented spectra was calibrated with the Fermi level of the sputter-cleaned Au substrate.

UPS spectra obtained during the C_{60} deposition on the ZnPc layer are shown in Fig. 1. The secondary electron cutoff positions (a) shift with the deposition of C_{60} , yielding a total 0.79 eV shift to lower binding energy. The valence region (b) shows the ZnPc characteristic emission features at the bottom spectrum, where the HOMO onset of the initial ZnPc is 1.08 eV. After depositing the C_{60} on it, the HOMO peak of ZnPc shifts to lower binding energy by 0.30 eV. The emission features of C_{60} emerge as the C_{60} thickness increases and the final film shows a HOMO onset of C_{60} at 1.90 eV. We evaluate that a total shift in the C_{60} HOMO is 0.43 eV toward the lower binding energy by following process. In order to estimate the accurate band shift of C_{60} during the layer formation, it is necessary to determine the HOMO position of C_{60} at the very first deposition stage. However, in this case, it is difficult to visualize the C_{60} HOMO feature due to the spectral overlap with the ZnPc emission features near 3.9 eV. Thus, we adopted a spectrum subtraction technique, giving the red dotted peak at 2.9 eV by subtracting the ZnPc spectrum from the C_{60} 0.4 nm spectrum. Therefore, the subtraction of sum of HOMO shifts (0.73 eV) from SE cutoff shift (0.79 eV) means 0.06 eV of interface dipole (eD) at bilayer interface. The ionization energy (IE) of ZnPc and C_{60} were determined to be 4.79 and 6.40 eV, respectively. [IE=(photon energy)-(SE cutoff)

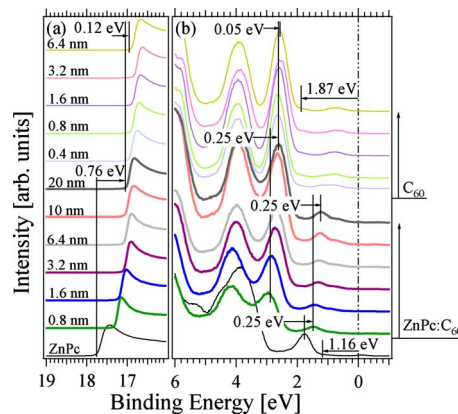


FIG. 2. (Color online) UPS spectra near the secondary cutoff region (a) the Fermi level and the Fermi level (b) the secondary cutoff region during the step-by-step layer deposition of ZnPc: C_{60} and C_{60} on the ZnPc layer. The HOMO shift of ZnPc is 0.50 eV, the shift of C_{60} is 0.25 eV and SE cutoff position is also moved 0.88 eV to lower binding energy.

+(HOMO onset)]. The IE of ZnPc and C_{60} are consistent with previously reported values¹²⁻¹⁴ within the margin of error of our measurements.

Figure 2 shows the UPS data obtained during the deposition of a ZnPc: C_{60} blended layer followed by C_{60} deposition. The SE cutoff positions (a) shift to the lower binding energy side by 0.76 eV during the ZnPc: C_{60} deposition and then shifts further to a lower binding energy by 0.12 eV with the subsequent C_{60} deposition. The HOMO onset position of the initial ZnPc layer is seen at 1.16 eV and the HOMO position moves to lower binding energy by 0.25 eV immediately after the deposition of the blended layer. When the thickness of the blended layer is increased, the ZnPc HOMO shifts further toward lower binding energies. The origin of this is energy level relaxation away from the blended layer/ZnPc interface. The C_{60} HOMO is also seen in the blended layer and is also relaxed toward the lower binding energy side by 0.25 eV, similar to the ZnPc HOMO. When the deposition of C_{60} on the blended layer is continued, the C_{60} HOMO shifts slightly by 0.05 eV and the final film shows a HOMO onset at 1.87 eV. (The small peak near 0.6 eV is the UV satellite peak of the C_{60} HOMO from the He $I\beta$ emission line.)

Finally, we obtained the energy level alignment at each interface, as shown in Fig. 3. The eD at each interface was

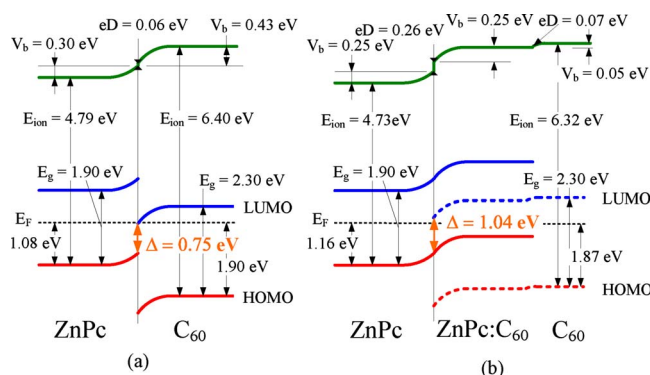


FIG. 3. (Color online) Energy level diagram of (a) C_{60} /ZnPc, (b) C_{60} /ZnPc: C_{60} /ZnPc. The offset between HOMO of ZnPc and LUMO of C_{60} which make V_{oc} are 0.75 eV for (a) and 1.04 eV for (b). C_{60} /ZnPc: C_{60} interface does not show any interaction.

estimated from the SE cutoff position and the HOMO level shifts. The SE cutoff shifts provide information on both the eD and the energy level shift, i.e., band bending (V_b), the two contributions need to be separated to accurately estimate the interface energy level alignment.¹⁵ As shown in Fig. 3(a), for the $C_{60}/ZnPc$ interface, the eD was estimated by subtracting the band bending of both layers from the total SE cutoff shift, yielding $eD=0.06$ eV. Band bending was obtained from the HOMO level shift of each layer and the values were determined to be 0.30 and 0.43 eV at the ZnPc and C_{60} layers, respectively. This band bending corresponds to the formation of a depletion layer in ZnPc and an accumulation layer in C_{60} due to charge transfer. Considering the accuracy of our measurement, there is no essentially eD. We used band gap values for ZnPc (1.9 eV) and C_{60} (2.3 eV) from previously reported studies^{16–18} in order to determine the LUMO position of each layer. The complete energy level alignment diagram is shown in Fig. 3(a) and the difference (Δ) between the donor HOMO and the acceptor LUMO is estimated to be 0.75 eV. This difference is regarded to the origin of V_{oc} of solar cells.¹⁹ Using the same approach, we obtained the energy level alignment at the $C_{60}/ZnPc:C_{60}/ZnPc$ interfaces, as shown in Fig. 3(b). The C_{60} energy level is indicated by a dotted line to indicate the blended layer. We determined the HOMO-LUMO difference (Δ) to be 1.04 eV which is about a 40% increase compared to that for a $C_{60}/ZnPc$ bilayer structure. Thus the blended structure results in a larger V_{oc} and, furthermore, the electron-hole pair generated in the blended layer can be more easily separated compared to that at the interface of a bilayer. This explains why the introduction of a blended structure improves the reported efficiencies of photovoltaic cells.¹⁶

The origin of the HOMO-LUMO difference (Δ) increase with a blended layer can be attributed to relatively small band bending and doping effects (electron transfer from ZnPc to C_{60}) at the ZnPc: $C_{60}/ZnPc$ interface. As mentioned above, the band bending corresponds to the formation of depletion layer in the donor and accumulation layer in the acceptor. Due to charge transfer, free holes and free electrons are accumulated in space charge layers. However, the electron carrier density in ZnPc: C_{60} layer is smaller than that in pure C_{60} layer because p-type ZnPc compensates the electron carrier. Therefore, less accumulation layer forms and smaller band bending occurs at the interface. As a result, due to the small band bending at the ZnPc: $C_{60}/ZnPc$ interface, the HOMO of C_{60} in the ZnPc: C_{60} layer is shifted further toward lower binding energies compared to the HOMO of C_{60} in the bilayer. Furthermore, doping effects are responsible for the relative shift between ZnPc HOMO and C_{60} LUMO. These two effects render a larger offset between donor (ZnPc) HOMO and acceptor (C_{60}) LUMO. As a result, the HOMO-LUMO difference (Δ), which is responsible for the V_{oc} in OPVs, increases.

In conclusion, we investigated the origin of the high power conversion efficient of OPVs with ZnPc and C_{60} as DA materials with different stack structures of bilayers and blended layers. By adopting a blended layer, charge redistribution occurs at the ZnPc: $C_{60}/ZnPc$ interface. As a result, the LUMO of C_{60} in the blended layer is at a higher position than that for the $C_{60}/ZnPc$ interface. This leads to a larger difference between the donor HOMO and the acceptor LUMO. From the complete energy level alignment at $C_{60}/ZnPc$ and $C_{60}/ZnPc:C_{60}/ZnPc$, we conclude that the difference between the donor HOMO and acceptor LUMO, which is responsible for the V_{oc} in OPVs, is increased by 0.29 eV. This is the main origin of the reported improved performance.

This work was supported by the IT R&D program of MKE/IITA (Grant No. 2008-F-023-01, next generation future device fabricated by using nanojunction) and New and Renewable Energy R&D program (Grant No: 2009T100100614) under the Ministry of Knowledge Economy, Republic of Korea.

¹A. Pochettino, *Acad. Lincei* **15**, 355 (1906).

²P. Peumans, A. Yakimov, and S. R. Forrest, *J. Appl. Phys.* **93**, 3693 (2003).

³C. J. Brabec, N. S. Sariciftci, and J. C. Hummelen, *Adv. Funct. Mater.* **11**, 15 (2001).

⁴J. Xue, S. Uchida, B. P. Rand, and S. R. Forrest, *Appl. Phys. Lett.* **84**, 3013 (2004).

⁵C. J. Brabec, A. Cravino, D. Meissner, N. Serdar Sariciftci, T. Fromherz, M. T. Rispens, L. Sanchez, and J. C. Hummelen, *Adv. Funct. Mater.* **11**, 374 (2001).

⁶J. Bouclé, P. Ravirajan, and J. Nelson, *J. Mater. Chem.* **17**, 3141 (2007).

⁷D. M. Nanditha, M. Dissanayake, A. A. D. T. Adikaari, R. J. Curry, R. A. Hatton, and S. R. P. Silva, *Appl. Phys. Lett.* **90**, 253502 (2007).

⁸B. Maennig, J. Drechsel, D. Gebeyehu, P. Simon, F. Kozlowski, A. Werner, F. Li, S. Grunmann, S. Sonntag, M. Koch, K. Leo, M. Pfeiffer, H. Hoppe, D. Meissner, N. S. Sariciftci, I. Riedel, V. Dyakonov, and J. Parisi, *Appl. Phys. A: Mater. Sci. Process.* **79**, 1 (2004).

⁹T. Taima, S. Toyoshima, K. Kara, K. Saito, and K. Yase, *Jpn. J. Appl. Phys., Part 2* **45**, L217 (2006).

¹⁰T. Taima, J. Sarai, T. Yamanari, and K. Saito, *Jpn. J. Appl. Phys., Part 2* **45**, L995 (2006).

¹¹R. Schlaf, B. A. Parkinson, P. A. Lee, K. W. Nebesny, and N. R. Armstrong, *J. Phys. Chem. B* **103**, 2984 (1999).

¹²T. Kimura, M. Sumimoto, S. Sakaki, H. Fujimoto, Y. Hashimoto, and S. Matsuzaki, *Chem. Phys.* **253**, 125 (2000).

¹³Y. Gassenbauer and A. Klein, *J. Phys. Chem. B* **110**, 4793 (2006).

¹⁴Y. Tanaka, K. Kanai, Y. Ouchi, and K. Seki, *Chem. Phys. Lett.* **441**, 63 (2007).

¹⁵H. Lüth, *Solid Surfaces, Interfaces, and Thin Films*, 4th ed. (Springer, New York, 2001), p. 537.

¹⁶W. Gao and A. Kahn, *Org. Electron.* **3**, 53 (2002).

¹⁷M. S. Golden, M. Knupfer, J. Fink, J. F. Armbruster, T. R. Cummins, H. A. Romberg, M. Roth, M. Sing, M. Schmidt, and E. Sohmen, *J. Phys.: Condens. Matter* **7**, 8219 (1995).

¹⁸R. W. Lof, M. A. Van Veenendaal, B. Koopmans, H. T. Jonkman, and G. A. Sawatzky, *Phys. Rev. Lett.* **68**, 3924 (1992).

¹⁹V. Dyakonov, *Physica E (Amsterdam)* **14**, 53 (2002).